Layered Material Exfoliation

International Edition: DOI: 10.1002/anie.201504693
German Edition: DOI: 10.1002/ange.201504693

A Kinetic Model for Exfoliation Kinetics of Layered Materials**

*John Texter**

Dedicated to Markus Antonietti

Abstract: *Exfoliation of two-dimensional materials is key to obtaining high-performance properties. We present a simple kinetic model for exfoliation that is readily solved analytically. Random and irreversible sheet separation is postulated in the presence of highly effective stabilizers. This model appears to quantitatively fit graphene exfoliation data, and it illuminates mechanistic aspects of exfoliation. Thicker sheets exfoliate much faster than trilayer and bilayer sheets. Exfoliation follows highly activated diffusion-controlled intercalation of stabilizer into inter-sheet galleries. Application to the most concentrated graphene exfoliation data available supports these assumptions and provides insight for practical treatment regimens.*

The synthesis and use of new layered materials[1–8] are becoming increasingly important in materials chemistry, and two-dimensional materials[9–15] have become a focal point in energy materials development. Layered fillers derived from natural and synthetic clays have become significant components in composite materials, and their exfoliation is an important mechanistic step in the formation of such materials.[16–22]

A prime candidate for exfoliation kinetic analysis is the much studied exfoliation of graphene.[23] Graphene, a unique two-dimensional allotrope of carbon,[24] has created great excitement in chemistry, physics, and materials science because of its high-performance electronic properties and its potential for transformational advances in optoelectronics[25] and plasmonic device development.[26,27] An important practical property of graphene is its relatively low cost[28] in comparison to its fullerene and carbon nanotube "cousins", in addition to its highly competitive electronic[29,30] and thermal transport properties.[31–33] High-volume applications in nanocomposites, inks, and devices such as batteries and sensors will require suitably formulated aqueous graphene dispersions, and much attention has been focused recently on the development of such dispersions.[34–37]

Although commercially available graphene aggregates and graphite (a very low-cost source of graphene) must be exfoliated to create stable and useful dispersions, and despite the importance of and interest[38–46] in such materials as well as of other layered materials, no quantitative kinetic model appears to have been disclosed for exfoliation. Here we present a kinetic model for exfoliation that is useful in helping us interpret exfoliation processing. This model should also provide utility in furthering exfoliation of topical materials, such as clays and other advanced layered compounds, in nanocomposite design.

We illustrate in Figure 1 recently reported[47] apparent optical density at 500 nm as a function of sonication time for two graphene-in-water dispersions, wherein the graphene weight concentration was 5%. These dispersions were stabilized using a (nanolatex) nanogel[48] derived[49,50] from a hydrophilic imidazolium acrylate monomer that also is an ionic liquid. The weight ratio of nanogel to graphene was 0.5.[47] This nanolatex material was measured by dynamic light scattering and found to be in the size range of 20–30 nm diameter (see Supporting Information (SI) for details). The apparent optical density, OD_{app}, was obtained by diluting a weighed aliquot of the dispersion with water sufficiently to obtain a measured optical density in the range of 0.1 to 1.5. This experimental value was then multiplied by the corresponding dilution factor (dilution weight/aliquot weight) to obtain OD_{app}. At short sonication times the OD_{app} is influenced by aggregate light scattering as well as by absorption. The relative contribution of non-absorbing scat-

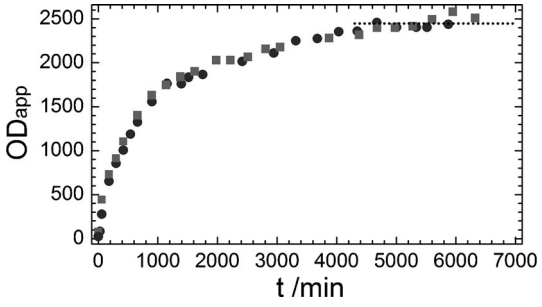

Figure 1. Apparent optical density at 500 nm of 5% aqueous graphene dispersion as a function of sonication time (●, initial preparation; ■, repeat); these values were obtained by diluting sufficiently to obtain absorbances < 2, followed by multiplying these absorbances by their respective dilution factors; adapted from Figure 3 of Ref. [47] with permission.

[*] Prof. Dr. J. Texter
School of Engineering Technology, Eastern Michigan University
Ypsilanti, MI 48197 (USA)
and
Department of Polymer Science and Engineering, College of Chemistry, Chemical Engineering and Materials Science, Soochow University, Suzhou 215123 (P.R. China)
E-mail: jtexter@emich.edu

[**] This paper was drafted while the author was a guest chair professor in the College of Chemistry, Chemical Engineering and Materials Science, Soochow University, Suzhou, PR China. The author thanks Professors Feng Yan and Hong Chen for their kind hospitality.

Supporting information for this article is available on the WWW under http://dx.doi.org/10.1002/anie.201504693.

tering decreases rapidly as exfoliation proceeds and true absorption dominates.

Imidazolium rings that do not contact the graphene are strongly hydrated and serve as dispersion-stabilizing components. We have found that in addition to nanolatex and triblock copolymer stabilization, linear random copolymers, homopolymers, as well as imidazolium bromide-based surfactants all are effective stabilizers for graphenic nano-objects in water.[51] The overall adsorbed polymer chains may be viewed as osmotic brushes that mitigate against indifferent salt-induced coagulation.[48]

The increase of OD_{app} as a function of time illustrated in Figure 1 suggests a model behavior that is similar to product accumulation in a first-order kinetic process. There is an initial rapid (exponential) rise followed by a much slower asymptotic increase. A plot of $OD_{app}(t)/OD_{app}(\infty)$ versus $t^{1/2}$ for these same data is illustrated in Figure 2, and there we see two distinct time intervals over which linear behavior is observed. The dispersion optical density of graphene exfoliation in NMP (*N*-methylpyrrolidone) was also reported to scale as $t^{1/2}$ by Coleman and co-workers.[35,52] An integral reaction–diffusion model for exfoliation of layered materials does not appear to be available, but intra-particle mass uptake of water and other sorbents has been found to exhibit linear uptake versus $t^{1/2}$ behavior for a variety of materials[53–56] and is assigned to adsorption–diffusion.

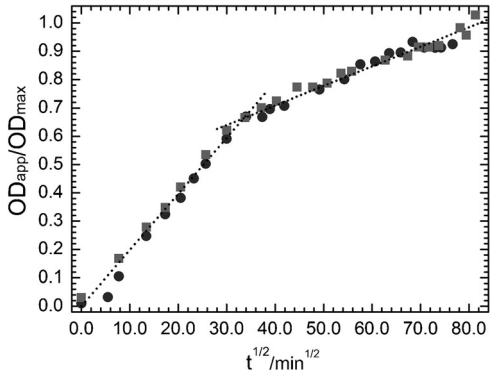

Figure 2. Evolution of exfoliation as a function of root time using the same data illustrated in Figure 1. The initial and final slopes are 0.0026 $s^{1/2}$ and 0.00086 $s^{1/2}$, respectively.

Intercalation–diffusion kinetics for Br_2 and HNO_3 uptake by graphite[57,58] yield diffusion coefficients of 5×10^{-10} cm^2s^{-1} to 6×10^{-8} cm^2s^{-1}. Somewhat slower diffusion is expected for polymer intercalation, and these aspects as they relate to the scaling of Figure 2 are discussed later. The slopes of the two domains illustrated in Figure 2 correspond to intra-platelet polymer (nanolatex) uptake.[56]

We adopt a model for consecutive first-order conversion of graphene platelets *m* sheets thick to pairs of thinner sheets. An *m*-sheet platelet has $m-1$ ways to split into an *r*-sheet and an *m*-*r*-sheet. Each such sheet can split further until only single sheets remain. Figure 3 illustrates five of the 12 ways a 13-sheet platelet can randomly split into *r* and $13-r$ sheets. In addition, we assume at this point that the rate constants, *k*, for splitting are the same, irrespective of platelet thickness or intra-platelet splitting position. We also assume that this splitting is random and irreversible. These assumptions are convenient for a first exposition. However, the model we derive can easily utilize empirically derived rate constants for particular steps.

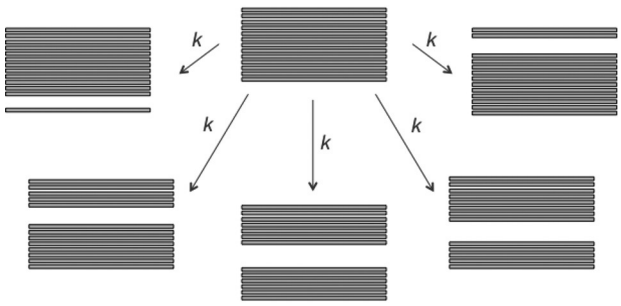

Figure 3. Illustration of five (of 12) ways a 13-sheet platelet can exfoliate into thinner pairs of sheets.

We adopt G_m as a variable for the number density of graphene *m*-sheets, and we can think of mG_m as a relative mass density of *m*-sheets. We assume the thickest sheets are set by $m=n$. The first-order rate for decomposition of each *m*-sheet is given by $-(m-1)kG_m$. Our irreversibility assumption limits *m*-sheet population growth to emanating from the decomposition of thicker *l*-sheets ($l=m+1, \ldots, n$). As can be seen in Figure 3, a given sheet thicker than an *m*-sheet will produce an *m*-sheet in a single step in two different ways. Further, a $2m$-sheet (even-numbered sheet) can only symmetrically split one way, but that way produces two *m*-sheets. A general rate equation for the number concentration of a G_m aggregate is then:

$$\frac{dG_m}{dt} = -(m-1)kG_m + 2k\sum_{l=m+1}^{n} G_l \qquad (1)$$

where *n* denotes the number of sheets in the thickest aggregates. This model conserves mass (see SI), and these effective rate constants, all integer multiples of *k*, follow from the above statistical argument based on assumed random irreversibility. In a case that rates for different types of splitting can be identified, empirically measured or theoretically derived rate constants can be inserted into this model without loss of generality.

All effects of stabilizer (polymer) concentration, temperature, mixing, sonication, etc., are embodied in the respective rate constants, as pseudo first-order constants. The chopping of larger areal sheets into smaller sheets is a well known aspect of graphene sonication,[47] and such processes are not considered in this model.

Exfoliation rates according to Equation (1) produce an upper triangular matrix of rate coefficients, for $m\geq2$, with eigenvalues: $k, 2k, 3k, 4k, \ldots, l_{max}k$. This kind of matrix follows from our assumption of irreversible exfoliation, wherein *m*-sheet platelets can only increase in number by exfoliation of thicker platelets. A particularly beneficial result of this assumption is that one can identify the system eigenvalues by inspection. The exfoliation of bilayers and trilayers represent the slowest steps of this mechanism.

The upper triangular nature of the system of differential equations defined by Equation (1) makes an analytical solution straightforward by the back-substitution method.[59] This method avoids having to invert the corresponding matrix of coefficients and can be obtained effectively algebraically (see SI). Once solutions for $G_2(t)$ to $G_n(t)$ are obtained, $G_1(t)$ is obtained by solving Equation (2):

$$\frac{dG_1}{dt} = 2k\sum_{l=2}^{n} G_l \qquad (2)$$

The general solution is simply given by $G_1(0)$ plus $2k$ times the sum over the time integrals of the $G_l(t)$.

A second and perhaps most significant aspect of this exfoliation mechanism is the gradual intercalation of stabilizing polymer between sheets. This process is activated by sonication, and when sufficient interlayer separation occurs, the newly available surface area is amenable to additional polymer adsorption. This process is illustrated between the top two sheets in the four-sheet platelet in Figure 4. There are

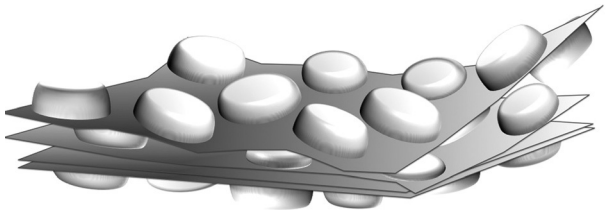

Figure 4. Cartoon depicting evolution of exfoliation of a four-sheet platelet illustrating outer surface saturation adsorption of nanolatex, intercalation of nanolatex between top and next sheets (left front), and intercalation–exfoliating adsorption of polymer on both surfaces between these same sheets (right).

two intermediate parts of such intercalation. A turbostatic situation[60] is illustrated in the left-front corner between these sheets where adsorbed polymer is attached to both upper and lower sheets. This kind of intermediate state was identified during studies of graphene aggregation wherein a bilayer had a monolayer of surfactant separating the two sheets.[60] On the right-hand side the adsorption has advanced so that polymer attached to upper and lower surfaces exhibits steric repulsion. When such adsorption onto opposing surfaces advances sufficiently, exfoliation occurs, such as in this cartoon where a 4-sheet separates into a 1-sheet and a 3-sheet. The activated penetration of polymer into these inter-sheet galleries is diffusion controlled and accounts for the $t^{1/2}$ behavior of Figure 2.

The large spread in specific time constants embodied in the model of Equation (1) suggests that a lot of exfoliation occurs during the earliest processing times. Thick sheets are predicted to separate much more quickly than thin sheets. Experimentally we see in Figure 1 that 20% of the eventually generated OD_{app} is achieved in about 90 min. We therefore recast these $OD_{app}(t)/OD_{max}$ data in the semilog format of Figure 5, and there we also see three distinct time intervals of behavior. Each linear domain exhibits a dominating first-order life-time (half-life). The long-time asymptote corresponds to a $\tau_{1/2}$ of 2660 min ($k = 6.03\times10^{-6}$ s), the middle interval yields a $\tau_{1/2}$ of 1110 min ($k = 1.45\times10^{-5}$ s), and the few data obtained in the first hour of sonication yield a $\tau_{1/2}$ of 370 min ($k = 4.32\times10^{-5}$ s). We stress that these rate constants are pseudo first-order constants that we expect are affected by polymer concentration, substrate concentration, dispersion viscosity, and sample treatment history. Further analyses of similar data sets may more fully elucidate effects of processing conditions on these rate constants.

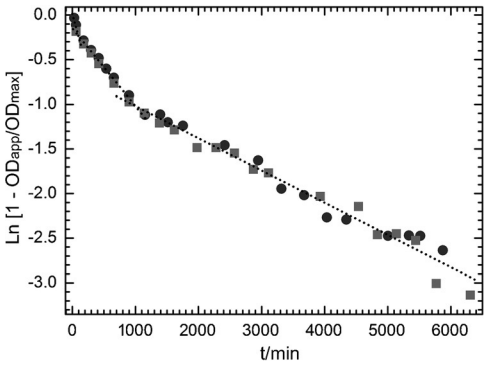

Figure 5. First-order rate constants and half-lives. The $\tau_{1/2}$ for $t < 100$ min is about 370 min, that for $100 < t < 1000$ min is about 1110 min, and that for the longer time interval is 2660 min.

The use of these experimentally derived rates in an appropriately modified version of Equation (1) is illustrated in the SI, along with associated "speciation" as a function of mass fraction. These time constants decrease by an approximate factor of 0.42 (half-life of 3-sheet/2-sheet) and 0.34 (half-life of 4-sheet/3-sheet), and if extrapolated yield half-lives for exfoliation of 0.96 min and 4.6×10^{-5} min, respectively, for 10-sheet and 20-sheet platelets. Half-lives for sequential platelet decompositions predicted from our equi-probable kinetic assumption decrease much more slowly, to 1/9 and to 1/19 that of 2-sheets for 10-sheet and 20-sheet platelets, respectively. We may therefore conclude that the exfoliation of graphene represented by the data of Figure 1 and Figure 5 proceeds much more rapidly than predicted by our equi-probable model.

The data of Figure 1, the scaling analysis of Figure 2, and the behavior illustrated in Figure 5 show that this exfoliation process may be viewed in terms of two domains, one occurring for $t < 1000$ min and one for longer t. If we take the geometric mean of the shortest lifetimes illustrated in Figure 5, 640 min, we see that the longest lifetime is about 4-fold longer. The scaling data in Figure 2 exhibit a three-fold ratio, and this ratio is in reasonable agreement with the more refined model of Figure 5.

Our kinetic argument that the data of Figure 1, Figure 2, and Figure 5 represent primarily the end stages of exfoliation to produce 3-sheet, 2-sheet, and single-sheet platelets appears supported by the accompanying speciation simulations (see SI). A series of layer-by-layer depositions of dilutions of one of the dispersions examined in Figure 1 produced up to 40 bilayers (the anionic adsorbate was sodium polystyrene sulfonate), and an optical density analysis of these coatings indicated on average that each bilayer contained 0.8 graphene

sheets.[47] This result independently supports our kinetic rate arguments and the illustrated speciation producing single sheet graphene by more than 90% by weight.

The variation in magnitude of absorption coefficients derived by other workers[47] supports our supposition that the absorption coefficient of graphene aggregates and of graphite flakes varies with thickness. While the fine structure constant component[61] of this visible absorption may not depend on thickness, it does seem likely that the $\pi \rightarrow \pi^*$ excitonic transition[62] would be prone to disruption by inter-sheet stacking. A full kinetic model would benefit greatly from independent determinations of absorption coefficients of graphene (and other layered materials) as a function of sheet thickness and relative light/sheet polarization.

In this introductory example we have used an effective optical density as a convenient kinetic observable. Optical studies of other inorganic layered materials, including MoS_2,[8,63–65] $MoSe_2$,[63,66] WS_2,[63,65] h-BN,[65,67] and $CuSbS_2$,[68] also appear to exhibit increases in visible absorbance with increasing degree of dispersion. However, in many cases such as in clays and silicates there may be too little visible absorbance to be useful, and another experimental observable will need to be examined. However, if the observable measured is a monotonic function of exfoliation degree, this simple model should be applicable. A proof of this concept is provided in the SI given that the measured property decreases (alternatively increases) with increasing platelet thickness.

A dynamical exfoliation model has been derived for highly activated exfoliation that is compatible with recently reported data for graphene exfoliated in water. An assumption of irreversible exfoliation, reasonable in the presence of good stabilizer, provides means to obtain analytical solutions. The equi-probable assumption of weak sensitivity of platelet decomposition on platelet thickness, helpful in deriving this pseudo first-order exfoliation model, is too slow to account for the experimental graphene data used in this report. Explicit data for thicker *m*-sheet lifetimes would be very helpful in understanding earlier-stage exfoliation of graphene.

Keywords: diffusion controlled intercalation · exfoliation · graphene · layered materials

How to cite: *Angew. Chem. Int. Ed.* **2015**, *54*, 10258–10262
Angew. Chem. **2015**, *127*, 10396–10400

[1] Q. H. Wang, K. Kalantar-Zadeh, A. Kis, J. N. Coleman, M. S. Strano, *Nat. Nanotechnol.* **2012**, *7*, 699–712.
[2] B. Zümreoglu-Karan, A. N. Ay, *Chem. Pap.* **2012**, *66*, 1–10.
[3] N. Miyamoto, T. Nakato, *Isr. J. Chem.* **2012**, *52*, 881–894.
[4] C. N. R. Rao, H. S. S. R. Matte, U. Maitra, *Angew. Chem. Int. Ed.* **2013**, *52*, 13162–13185; *Angew. Chem.* **2013**, *125*, 13400–13424.
[5] V. Nicolosi, M. Chhowalla, M. G. Kanatzidis, M. S. Strano, J. N. Coleman, *Science* **2013**, *340*, 1226419.
[6] N. Baliarsingh, K. M. Parida, G. C. Pradhan, *RSC Adv.* **2013**, *3*, 23865–23878.
[7] R. Ganatra, Q. Zhang, *ACS Nano* **2014**, *8*, 4074–4099.
[8] B. D. Mao, Y. B. Yuan, Y. C. Shao, B. Yang, Z. G. Xiao, J.-S. Huang, *Nanosci. Nanotech. Lett.* **2014**, *6*, 685–691.
[9] G. P. Wang, L. Zhang, J. J. Zhang, *Chem. Soc. Rev.* **2012**, *41*, 797–828.
[10] X. Huang, X. Y. Qi, F. Boey, H. Zhang, *Chem. Soc. Rev.* **2012**, *41*, 666–686.
[11] N. S. Choi, Z. H. Chen, S. A. Freunberger, X. L. Ji, Y. K. Sun, K. Amine, G. Yushin, L. F. Nazar, J. Cho, P. G. Bruce, *Angew. Chem. Int. Ed.* **2012**, *51*, 9994–10024; *Angew. Chem.* **2012**, *124*, 10134–10166.
[12] A. B. Laursen, S. Kegnaes, S. Dahl, I. Chorkendorff, *Energy Environ. Sci.* **2012**, *5*, 5577–5591.
[13] M. S. Xu, T. Liang, M. M. Shi, H. Z. Chen, *Chem. Rev.* **2013**, *113*, 3766–3798.
[14] D. Jariwala, V. K. Sangwan, L. J. Lauhon, T. J. Marks, M. C. Hersam, *ACS Nano* **2014**, *8*, 1102–1120.
[15] M. Q. Zhang, M. Sedran, Z. Ling, M. R. Lukatskaya, O. Mashtalir, M. Ghidiu, B. Dyatkin, D. J. Tallman, T. Djecizian, M. W. Barsourn, Y. Gogotsi, *Angew. Chem. Int. Ed.* **2015**, *54*, 4810–4814; *Angew. Chem.* **2015**, *127*, 4892–4896.
[16] D. R. Paul, L. M. Robeson, *Polymer* **2008**, *49*, 3187–3204.
[17] S. Pavlidou, C. D. Papaspyrides, *Prog. Polym. Sci.* **2008**, *33*, 1119–1198.
[18] G. Choudalakis, A. D. Gotsis, *Eur. Polym. J.* **2009**, *45*, 967–984.
[19] I. Nicotera, A. Enotiadis, K. Angjeli, L. Coppola, *Int. J. Hydrogen Energy* **2012**, *37*, 6236–6245.
[20] M. Yi, Z. G. Shen, W. Zhang, J. Y. Zhu, L. Liu, S. S. Liang, X. J. Zhang, S. L. Ma, *Nanoscale* **2013**, *5*, 10660–10667.
[21] B. M. Mosby, A. Diaz, V. Bakhmutov, A. Clearfield, *ACS Appl. Mater. Interfaces* **2014**, *6*, 585–592.
[22] C. Rubio, B. Zomoza, P. Gorgojo, C. Tellez, J. Coronas, *Curr. Org. Chem.* **2014**, *18*, 2351–2363.
[23] J. Texter, *Curr. Opin. Colloid Interface Sci.* **2014**, *19*, 163–174.
[24] A. K. Geim, K. S. Novoselov, *Nat. Mater.* **2007**, *6*, 183–191.
[25] P. Avouris, Z. H. Chen, V. Perebeinos, *Nat. Nanotechnol.* **2007**, *2*, 605–615.
[26] F. Bonaccorso, Z. Sun, T. Hasan, A. C. Ferrari, *Nat. Photonics* **2010**, *4*, 611–612.
[27] Z. Y. Xia, S. Pezzini, E. Treossi, G. Giambastiani, F. Corticelli, V. Morandi, A. Zanelli, V. Bellani, V. Palermo, *Adv. Funct. Mater.* **2013**, *23*, 4684–4693.
[28] A. A. Green, M. C. Hersam, *Nano Lett.* **2009**, *9*, 4031–4036.
[29] A. H. Castro Neto, F. Guinea, N. M. R. Peres, K. S. Novoselov, A. K. Geim, *Rev. Mod. Phys.* **2009**, *81*, 109–162.
[30] Z. Yang, R. G. Gao, N. T. Hu, J. Chai, Y. W. Cheng, L. Y. Zhang, H. Wei, E. S. W. Kong, Y. F. Zhang, *Nano-Micro Lett.* **2012**, *4*, 1–9.
[31] S. Ghosh, W. H. Bao, D. L. Nika, S. Subrina, E. P. Pokatilov, C. N. Lau, A. A. Balandin, *Nat. Mater.* **2010**, *9*, 555–558.
[32] J. H. Seol, I. S. Jo, A. Moore, L. Lindsay, Z. H. Aitken, M. T. Pettes, X. S. Li, Z. Yao, R. Huang, D. Broidao, N. Mingo, R. S. Ruoff, L. Shi, *Science* **2010**, *328*, 213–216.
[33] M. M. Sadeghi, M. T. Pettes, L. Shi, *Solid State Commun.* **2012**, *152*, 1321–1330.
[34] R. Ruoff, *Nat. Nanotechnol.* **2008**, *3*, 10–11.
[35] J. N. Coleman, *Acc. Chem. Res.* **2013**, *46*, 14–22.
[36] D. Joseph, S. Seo, D. R. Williams, K. E. Geckeler, *ACS Appl. Mater. Interfaces* **2014**, *6*, 3347–3356.
[37] Z. Y. Sun, J. Vivekananthan, D. A. Guschin, X. Huang, V. Kuznetsov, P. Ebbinhaus, A. Sarfraz, M. Muhler, W. Schuhmann, *Chem. Eur. J.* **2014**, *20*, 5752–5761.
[38] P. Laaksonen, M. Kainlauri, T. Laaksonen, A. Shchepetov, H. Jiang, J. Ahopelto, M. B. Linder, *Angew. Chem. Int. Ed.* **2010**, *49*, 4946–4949; *Angew. Chem.* **2010**, *122*, 5066–5069.
[39] M. Du, X. L. Li, A. Z. Wang, Y. Z. Wu, X. P. Hao, M. W. Zhao, *Angew. Chem. Int. Ed.* **2014**, *53*, 3645–3649; *Angew. Chem.* **2014**, *126*, 3719–3723.
[40] H. S. S. Ramakrishna Matte, A. Gomathi, A. K. Manna, D. J. Late, S. K. Pat, C. N. R. Rao, *Angew. Chem. Int. Ed.* **2010**, *49*, 4059–4062; *Angew. Chem.* **2010**, *122*, 4153–4156.

[41] Z. Y. Zeng, T. Sun, J. X. Zhu, X. Huang, Z. Y. Yin, G. Lu, Z. X. Fan, Q. Y. Yan, H. Hoon Hng, H. Zhang, *Angew. Chem. Int. Ed.* **2012**, *51*, 9052 – 9056; *Angew. Chem.* **2012**, *124*, 9186 – 9190.
[42] A. Ciesielski, S. Haar, M. El Gemayel, H. F. Yang, J. Clough, G. Melinte, M. Gobbi, E. Orgiu, M. V. Nardi, G. Ligorio, V. Palermo, N. Koch, O. Ersen, C. Casiraghi, P. Samor, *Angew. Chem. Int. Ed.* **2014**, *53*, 10355 – 10361; *Angew. Chem.* **2014**, *126*, 10523 – 10529.
[43] K. Xu, P. Z. Chen, X. L. Li, C. Z. Wu, Y. Q. Guo, J. Y. Zhao, X. J. Wu, Y. Xie, *Angew. Chem. Int. Ed.* **2013**, *52*, 10477 – 10481; *Angew. Chem.* **2013**, *125*, 10671 – 10675.
[44] K. G. Zhou, N. N. Mao, H. X. Wang, Y. Peng, H. L. Zhang, *Angew. Chem. Int. Ed.* **2011**, *50*, 10839 – 10842; *Angew. Chem.* **2011**, *123*, 11031 – 11034.
[45] Z. Y. Zeng, Z. Y. Yin, X. Huang, H. Li, Q. Y. He, G. Lu, F. Boey, H. Zhang, *Angew. Chem. Int. Ed.* **2011**, *50*, 11093 – 11097; *Angew. Chem.* **2011**, *123*, 11289 – 11293.
[46] K. R. Paton, E. Varrla, C. Backes, R. J. Smith, U. Khan, A. O'Neill, C. Boland, M. Lotya, O. M. Istrate, P. J. King, et al., *Nat. Mater.* **2014**, *13*, 624 – 630.
[47] D. Ager, V. Arjunan Vasantha, R. Crombez, J. Texter, *ACS Nano* **2014**, *8*, 11191 – 11205.
[48] D. England, N. Tambe, J. Texter, *ACS Macro Lett.* **2012**, *1*, 310 – 314.
[49] F. Yan, J. Texter, *Chem. Commun.* **2006**, 2696 – 2698.
[50] F. Lu, F. Yan, J. Texter, *Prog. Polym. Sci.* **2009**, *34*, 431 – 448.
[51] J. Texter, US Patent 8,920,682, December 30, **2014**.
[52] U. Khan, A. O'Neil, M. Loyta, S. De, J. N. Coleman, *Small* **2010**, *6*, 864 – 871.
[53] S. H. Anderson Axdal, D. D. L. Chung, *Carbon* **1987**, *25*, 191 – 210.
[54] H. Dalir, R. D. Farahani, V. Nhim, B. Samson, M. Levesque, D. Therriault, *Langmuir* **2012**, *28*, 791 – 803.
[55] V. Bugatti, U. Costantino, G. Gorrasi, M. Nocchetti, L. Tammaro, V. Vittoria, *Eur. Polym. J.* **2010**, *46*, 418 – 427.
[56] K. Shakir, H. F. Ghoneimy, I. T. Hennawy, A. F. Elkafrawy, S. G. E. Beheir, M. Refaat, *Eur. J. Chem.* **2011**, *2*, 83 – 93.
[57] M. B. Dowell, D. S. Badorrek, *Carbon* **1978**, *16*, 241 – 249.
[58] S. A. Solin in *Intercalation in Layered Materials* (Ed.: M. Dresselhaus), Springer, New York, **1986**, pp. 173 – 183; *NATO ASI Series* **1986**, *148*, 173 – 183.
[59] J. K. Reid, J. A. Scott, *ACM Trans. Math. Software* **2011**, *38*, 10.
[60] S. C. Lin, C. J. Shih, M. S. Strano, D. Blankschtein, *J. Am. Chem. Soc.* **2011**, *133*, 12810 – 12823.
[61] R. R. Nair, P. Blake, A. N. Grigorenko, K. S. Novoselov, T. J. Booth, T. Stauber, N. M. R. Peres, A. K. Geim, *Science* **2008**, *320*, 1308 – 1308.
[62] J. W. Weber, V. E. Calado, M. C. M. van de Sanden, *Appl. Phys. Lett.* **2010**, *97*, 091904.
[63] G. Cunningham, M. Loyta, C. S. Cucinotta, S. Sanvito, S. D. Bergin, R. Menzel, M. S. P. Shaffer, J. N. Coleman, *ACS Nano* **2012**, *6*, 3468 – 3480.
[64] Q. H. Wang, K. Kalantar-Zadeh, A. Kis, J. N. Coleman, M. S. Strano, *Nat. Nanotechnol.* **2012**, *7*, 699 – 712.
[65] L. Guardia, J. I. Paredes, R. Rozada, S. Villar-Rodil, A. Martinez-Alonso, J. M. D. Tascon, *RSC Adv.* **2014**, *4*, 14115 – 14127.
[66] MoSe2 X. Zhang, Z. C. Lai, Z. D. Liu, C. L. Tan, Y. Huang, B. Li, M. T. Zhao, L. H. Xie, W. Huang, H. Zhang, *Angew. Chem. Int. Ed.* **2015**, *54*, 5425 – 5428; *Angew. Chem.* **2015**, *127*, 5515 – 5518.
[67] L. Cao, S. Emami, K. Lafdi, *Mater. Express* **2014**, *4*, 165 – 171.
[68] K. Ramasamy, H. Sims, W. H. Butler, A. Gupta, *J. Am. Chem. Soc.* **2014**, *136*, 1587 – 1598.

Received: May 24, 2015
Revised: June 11, 2015
Published online: July 14, 2015

